Optimization-free fast charging for lithium-ion batteries using model inversion techniques

(article starts on next page)

Optimization-Free Fast Charging for Lithium-Ion Batteries Using Model Inversion Techniques

Yang Li, **Torsten Wik**, **Yicun Huang**, **Changfu Zou**

*Chalmers University of Technology, Gothenburg, 41296, Sweden
(e-mail: yangli@ieee.org, tw@chalmers.se, yicun@chalmers.se,
changfu.zou@chalmers.se).*

Abstract: We propose a novel fast-charging control framework for lithium-ion (Li-ion) batteries that can leverage a class of models including the high-dimensional, electrochemical-thermal pseudo-two-dimensional model. The control objective is to find the highest battery current while fulfilling various operating constraints. Conventionally, computationally demanding optimization is needed to solve such a constrained optimal control problem when an electrochemical-thermal model is used, leading to practical difficulties in achieving low-cost implementation. Instead, this paper provides an optimization-free solution to Li-ion battery fast charging by converting the constrained optimal control problem into an output tracking problem with multiple tracking references. The required control input, i.e., the charging current, is derived by inverting the battery model. As a result, a nonlinear inversion-based control algorithm is obtained for Li-ion battery fast charging. Results from comparative studies show that the proposed controller can achieve performance close to nonlinear model predictive control but at significantly reduced computational costs and parameter tuning efforts.

1. INTRODUCTION

Long charging times are a notorious issue for lithium-ion (Li-ion) battery-powered electric vehicles (EVs), which can cause long queues at the charging station and serious road congestion nearby, especially as the EV adoption level increases. Currently, conservative low-to-medium charging rates are often applied, including commercially-viable charging protocols such as constant-current constant-voltage (CC-CV), constant-power constant-voltage (CP-CV), multistage CC, and boost charging (see, e.g., Notten et al. (2005); Liu and Luo (2010); Chen et al. (2013)). These model-free and heuristic methods are characterized by predefined profiles with limited patterns on constant current, voltage, and/or power, while the internal dynamics of the battery are not used for the design due to a lack of relevant domain knowledge. Increasing the charging current rates under these conditions will speed up the battery aging, cause damage, and even pose severe hazards to EV users.

Various battery models can provide the required internal information, which can be used to design model-based charging strategies. Conventionally, lumped-parameter equivalent circuit models (ECMs) with simple circuit structures are used, and the state of charge (SOC), state of health (SOH), and internal temperature are used to design charging strategies based on frequency optimization (Lee and Park (2015)), multi-objective optimization (Wang and Liu (2015)), fuzzy control, or model predictive control (MPC) (Zou et al. (2017)). On the other hand, physics-based

models have recently been investigated for the design of fast charging algorithms.

Physics-based models can accurately reproduce electrochemical battery dynamics, such as ion diffusion, intercalation kinetics, and heat generation and transfer (Li et al. (2019)). Based on physics-based models, optimization problems and open-loop optimal controls have been formulated to minimize charging duration (Pramanik and Anwar (2016)). A few charging strategies equipped with closed-loop control algorithms were recently proposed. For instance, a fast-charging strategy was developed utilizing an isothermal electrochemical model, health-related constraints, and nonlinear MPC (NMPC) (Liu et al. (2017)). A one-step NMPC was proposed to optimize charging profiles by incorporating thermal dynamics into a multi-physics pseudo-two-dimensional (P2D) model described by partial-differential-algebraic equations (PDAEs) (Klein et al. (2011)). However, the applications are largely limited by their intractable computations associated with nonlinear PDAE models and nonlinear online optimization unless a very large time step is adopted at the expense of reduced accuracy. To solve the problem of low computational efficiency, a linear time-varying MPC (LTV-MPC) was proposed based on a reduced-order model (ROM) of Li-ion battery (Zou et al. (2018)), where the nonuniform effect over the electrode thickness was ignored. To develop the ROMs, most existing fast charging strategies assume that the battery behaviors are uniform over each electrode, which can significantly reduce the modeling and computational complexity (Li et al. (2021a)).

However, ignoring the nonuniformity in Li-ion battery electrodes can lead to inaccurate prediction of battery degradation, especially under fast charging scenarios. For instance, the spatially uneven development of lithium plating and the solid-electrolyte interphase (SEI) film can be observed, and the phenomena can be significantly exacerbated under extremely high charge current conditions due to certain chain effects (Yang and Wang (2018)). Significant model errors due to the uniform assumptions can make the designed control scheme too aggressive, especially for high-energy battery cells with thick electrodes (Boyce et al. (2021)). To address this problem, well-established spatial discretization methods, such as finite volume method (FVM), can be generally applied to simplify the multi-physics PDAE model, so that the spatially distributed dynamics can be accurately captured. By Li et al. (2019), the model is reformulated as a multi-physics distributed-parameter circuit network to overcome the major drawbacks of the existing *ad-hoc* ROMs. Some initial attempts have been made to develop NMPC-based fast charging strategies using such a high-dimensional model, showing its prospect for future implementation (see e.g., Pozzi et al. (2020)).

Unfortunately, high-dimensional nonlinear systems are fundamentally difficult to be used for control algorithms that require online optimization, such as LTV-MPC and NMPC. To sidestep the computational problems, in this work, we propose a model-based nonlinear control strategy based on the inversion technique for battery charging. We show that the variables in the P2D model, or their first time-derivatives, can be expressed as an affine-input or a quadratic-input form. This fact motivates us to derive analytical solutions so that the required input charging current can be analytically calculated using the high-fidelity battery model in different operating modes, and thus the charging current will meet all constraints. Consequently, the original constrained optimal control problem is converted to a multiple-output tracking problem. The proposed optimization-free nonlinear inversion-based output tracking control strategy requires almost no parameter tuning efforts and is shown to largely outperform MPC-based methods in terms of computational efficiency.

2. INVERSION-BASED CONTROL FOR BATTERY FAST CHARGING

2.1 General Problem Statement and Optimization-Based Solution for Battery Fast Charging

The general problem of optimal battery fast charging has been well-discussed by Klein et al. (2011) and can be cast as a time-optimal control problem. Let SOC_0 be a low initial charge level at time $t = 0$ and SOC_f as a high target charge level at $t = t_f$. Suppose the battery is charging from a given initial state x_0 at $t = 0$, but the end of charging is not specified (as a variable end-point problem). The optimal fast charging solution is obtained by solving

Problem 1 (General Fast Charging Problem):

$$\min_{u(t), t \in [0, t_f]} \int_0^{t_f} 1 \, dt \tag{1a}$$

$$\text{s.t.} \quad \text{state equation} \quad \dot{x}(t) = f(x(t), u(t)), \tag{1b}$$

output equation $\quad y(t) = g(x(t), u(t)),$ $\quad$ (1c)

initial state $\quad x(0) = x_0,$ $\qquad\qquad$ (1d)

final SOC $\quad SOC(t_f) = SOC_f,$ $\qquad$ (1e)

inequality constraints $\quad y(t) \leq y^*,$ $\quad$ (1f)

where $x \in \mathbb{R}^{n_x}$ is the state vector and the battery charging current $u = I_{app} \in \mathbb{R}^+$ is the single input (We define the current as positive during charging). $f : \mathbb{R}^{n_x} \times \mathbb{R} \to \mathbb{R}^{n_x}$ and $g : \mathbb{R}^{n_x} \times \mathbb{R} \to \mathbb{R}^{n_y}$ are two nonlinear operators on x and u. The battery SOC usually can be expressed as a linear function of state x (e.g., x contains concentration terms or SOC itself). Furthermore, y is a generalized output vector and its elements include all health- and safety-related variables that can limit battery charging rates. These can include either the external variables such as current, voltage, and power, as well as internal variables such as battery temperature, concentrations, side-reaction potential, etc (See Section 3.2). Here, we use y_j, y_j^*, and g_j to denote the jth element of y, y^*, and g, respectively, where $j \in \{1, 2, \cdots, n_y\}$. Note that in contrast to the common formulation in the literature, we treat the system input u as an output and the first element of the output y, i.e., $y_1 = u$ and $y_1^* = \overline{u}$, where $\overline{u}$ is the upper limit of the input.

Unfortunately, as discussed by Klein et al. (2011), this general fast charging problem is difficult to solve analytically as the battery model is usually highly nonlinear and subject to many state/output constraints. However, based on numerically obtained approximated global solution, Klein et al. (2011) shows that Problem 1 can be well addressed via NMPC, i.e., at each control instance $t \in [0, \Delta t, 2\Delta t, \cdots, t_f - \Delta t]$ the following nonlinear optimization problem with a reduced prediction horizon $[t, t + H]$ is solved:

Problem 2 (NMPC-Based Fast Charging):

$$u^\star(\tau) = \arg\min_{u(\tau), \tau \in [t, t+H]} -\int_t^{t+H} u(\tau) d\tau \tag{2}$$

$$\text{s.t.} \quad \text{the same constraints as (1b)--(1f).}$$

Only a segment of the obtained solution $u^\star(\tau), \tau \in [t, t + \Delta t]$ is implemented. Problem 2 is repeatedly solved starting from the new current state so that new control input is calculated and implemented.

2.2 Inversion-Based Output Tracking

For the fast charging problem under the conditions of extremely high current and wide temperature ranges, considerable nonuniform battery dynamics can be excited so that a high-dimensional nonlinear model is essential to guarantee the prediction accuracy. For short prediction horizons, the fast charging problem (2) can also be solved via the LTV-MPC. However, in the presence of hundreds of battery cells in a battery pack, the cell inconsistency problem needs also to be properly addressed when designing the control algorithm. In this condition, the complexity and computational burden of an MPC solver for battery systems may increase dramatically.

To cope with this challenge, we first consider a relaxed problem similar to Problem 2, but with only the first (regarding the input) and the jth inequality constraints of

(1f) imposed. We denote this problem as Problem 3.j. For Problem 3.1 where only the input constraint is imposed, we have

Problem 3.1 (Input-Bounded Fast Charging):

$$u^\star(t) = \underset{u(t),t\in[t_k,t_k+H]}{\arg\min} -\int_{t_k}^{t_k+H} u(t)dt \qquad (3a)$$

$$\text{s.t. the same constraints as (1b)–(1e),}$$
$$u(t) \le \overline{u}. \qquad (3b)$$

We can immediately obtain the solution as $u(t) \equiv \overline{u}$. The corresponding charging time can be approximated as $3600\mathcal{Q}_{\max}(\mathrm{SOC}_f - \mathrm{SOC}_0)/(\eta\overline{u})$ given by coulomb counting

$$\dot{\mathrm{SOC}}(t) = \eta I_{\mathrm{app}}(t)/(3600\mathcal{Q}_{\max}), \qquad (4)$$

where η is the coulombic efficiency and $\mathcal{Q}_{\max}$ is the battery capacity in ampere-hour (Ah).

Next, consider Problem 3.j where $j \in \{2, 3, \cdots\}$, i.e.,

Problem 3.j (Input-Output-Bounded Fast Charging):

$$u^\star(t) = \underset{u(t),t\in[t_k,t_k+H]}{\arg\min} -\int_{t_k}^{t_k+H} u(t)dt \qquad (5a)$$

$$\text{s.t. the same constraints as (1b)–(1e),}$$
$$u(t) \le \overline{u}, \qquad (5b)$$
$$y_j(t) \le y_j^*. \qquad (5c)$$

In this case, one more constraint is imposed along with the input constraint, and thus, the corresponding optimal current is always less or equal to that of Problem 3.1. In other words, the optimal solution to Problem 3.j should always be in the feasible domain of Problem 3.1. In this condition, to guarantee the compliance of the inequality constraints, the optimal output should always track one of the upper bounds y_j^*. We thus propose to design a simple control strategy as

$$I_{\mathrm{app}}^*(t) = u^*(x(t), y_1^*, y_2^*, \cdots)$$
$$\equiv \min\{u_j^*(x(t), y_j^*) \mid j = 1, \cdots, n_y\}, \qquad (6)$$

where u_j^* is the solution for the output y_j to track its reference or constraint y_j^*. This general control strategy converts an optimal control problem to an output tracking problem with multiple tracking objectives y_j^*, where we should apply the lowest current to charge the battery.

Inversion-based techniques will now be used to solve the output tracking problem (Devasia et al. (1996)). As will be shown in the latter sections, all the output variables in the present investigation can be expressed in low-degree input-polynomial forms. Based on this fact, we will analyze and derive a control strategy based on whether the input u has direct feedthrough to the output y_j or not. For brevity, the time argument t will be dropped henceforth.

2.3 Input With Direct Feedthrough to the Output

If the input u has a direct feedthrough to an output y_j and that y_j can be written as a polynomial function of u, and coefficients of the polynomial only depend on x

$$y_j = g_j(x,u) = \sum_{l=0}^{L_j} h_j^{[l]}(x)u^l$$
$$= h_j^{[0]}(x) + h_j^{[1]}(x)u + \cdots + h_j^{[L_j]}(x)u^{L_j}, \qquad (7)$$

where $h_j^{[l]} : \mathbb{R}^{n_x} \to \mathbb{R}$ represents the lth coefficient (function) for the jth output variable, $L_j \in \mathbb{Z}^+$ represents the degree of the polynomial, and $\mathbb{Z}^+$ represents a set of all positive integers. We note that $h_j^{[l]}$ is a state-dependent coefficient (SDC).

Given the reference output $y_j = y_j^*$, we seek the solution $u = u_j^* = g_j^{-1}(x, y_j^*)$, based on (7), by inversion. Analytical solutions exist and are easy to obtain for a low-degree polynomial. For example, when $L_j = 1$, namely $h_j^{[1]}(x) \ne 0$, (7) becomes input-affine, and the required control input u_j^* is

$$u_j^* = \frac{y_j^* - h_j^{[0]}(x)}{h_j^{[1]}(x)}. \qquad (8)$$

When the input u itself is considered an output variable, then $h_j^{[0]}(x) \equiv 0$ and $h_j^{[1]}(x) \equiv 1$.

If $L_j = 2$, $h_j^{[2]}(x) \ne 0$, (7) becomes an input-quadratic form. For the charging process, given $y_j = y_j^*$, the required input is the nonnegative solution to a quadratic equation, i.e.,

$$u_j^* = \frac{-h_j^{[1]}(x) + \sqrt{(h_j^{[1]}(x))^2 - 4h_j^{[2]}(x)(h_j^{[0]}(x) - y_j^*)}}{2h_j^{[2]}(x)}. \qquad (9)$$

For $L_j = 3$, the analytical solution exists, although the expression is rather complex. When $L_j > 3$, there are no general analytical solutions (Moulay and Perruquetti (2005)). Fortunately, we will show that input-polynomial forms with $L_j \ge 3$ are not needed in the present study on battery charging control.

2.4 Input Without Direct Feedthrough to the Output

It should be noted that if $L_j = 0$ in (7), the input has no direct feedthrough to the output, and thus the output will be a function of the states x only. In this condition, instead of investigating (7), we consider the first time-derivative of y_j. Similarly to (7), we assume $\dot{y}_j$ can be expressed in an input-polynomial form, i.e.,

$$\dot{y}_j = \dot{g}_j(x,u) = \sum_{l=0}^{L_j} h_j^{[l]}(x)u^l, \qquad (10)$$

where $L_j \in \mathbb{Z}^+$.

Clearly, to achieve $y_j = y_j^*$ at all times, a direct inversion of the input-output relationship (10) requires unfavorable differential operation for practical implementation. To avoid the differential operation and achieve zero-offset control, we propose to shape the relationship between y_j^* and y_j as a first-order system with a unit gain, i.e.,

$$\tau_j \dot{y}_j = -y_j + y_j^*, \qquad (11)$$

where the time constant τ_j is a tuning parameter. In this way, the output variable can exponentially approach its upper bound in a monotonic manner without generating an overshoot. Substituting (10) into (11) yields

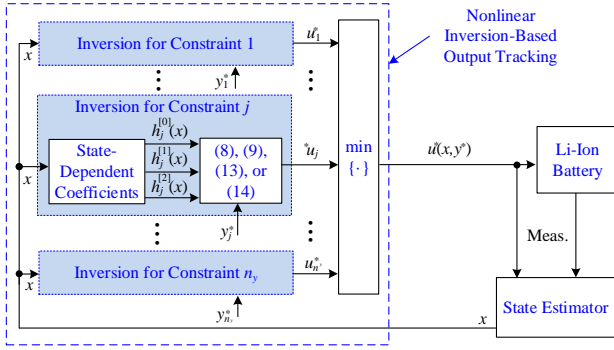$$\frac{y_j^* - y_j(x)}{\tau_j} = \sum_{l=0}^{L_j} h_j^{[l]}(x)u^l. \qquad (12)$$

Fig. 1. Block diagram of the proposed nonlinear inversion-based output tracking for fast charging control of Li-ion batteries

One can then solve (12) for u based on the polynomial degree L_j, and similar results to (8) and (9) can be obtained. Specifically, if $L_j = 1$, (10) possesses an input-affine form, and the required control input is

$$u_j^* = \frac{\frac{y_j^* - y_j(x)}{\tau_j} - h_j^{[0]}(x)}{h_j^{[1]}(x)}. \tag{13}$$

If $L_j = 2$, (10) has an input-quadratic form, and the required nonnegative control input for battery charging is

$$u_j^* = \frac{-h_j^{[1]}(x) + \sqrt{(h_j^{[1]}(x))^2 - 4h_j^{[2]}(x)(h_j^{[0]}(x) - \frac{y_j^* - y_j(x)}{\tau_j})}}{2h_j^{[2]}(x)}. \tag{14}$$

2.5 Overall Control Framework

The proposed inversion-based charging control strategy is illustrated in Fig. 1. Here, the inversion-based control essentially calculates the feedforward (FF) component u^* as a nonlinear function of the state x and all output references/constraints y_j^*. $u^*(\cdot)$, and use it as the nominal tracking control command. This FF control assumes precise prior knowledge of the battery model is available (Devasia (2002)). Note that the state x requires to be fully observable in this strategy. For a high-dimensional nonlinear battery model, a battery state estimator based on ensemble-based methods, such as the ensemble Kalman filter (Li et al. (2021c)) and the singular evolutive intepolated Kalman filter (Li et al. (2022)), can be designed to reduce computational costs. However, state estimation will not be elaborated in the present work for the sake of brevity. We assume direct access to the system state x is available. Although not demonstrated in the work, it is easy to show that common physical quantities in a battery, such as potentials/voltages, currents, concentrations, molar fluxes, temperature, and power, can be tracked using the proposed inversion method.

3. ILLUSTRATIVE EXAMPLES

3.1 System Configuration

In this section, results from simulation studies will be presented to verify the efficacy of the proposed con-
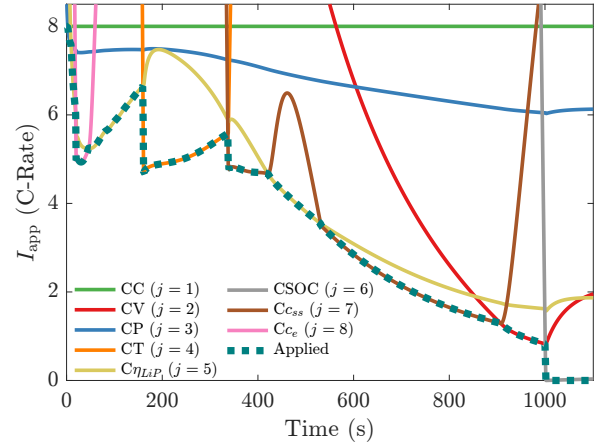

Fig. 2. Construction of the charging current profile limited by various physical constraints. CC: constant current; CV: constant voltage; CP: constant power; Cη_{LiP}: constant lithium plating potential; CT: constant temperature; CSOC: constant SOC; Cc_{ss}: constant solid-phase surface concentration; Cc_e: constant electrolyte concentration

trol strategy using an electrochemical-thermal pseudo-two-dimensional model (P2D-T). The battery model and controller are both implemented in MATLAB R2016a, and the simulated results were obtained on a 64-bit Windows 10 on a PC with Intel Core 2 Q9400 @ 2.67GHz processor and 8GB RAM. To simulate the plant, we consider evenly divided control volumes in each domain in an FVM scheme, and the numbers of control volumes of the battery model are selected to be high (10, 3, 10 for the positive electrode, separator, and negative electrode, respectively) to guarantee the model fidelity under high-current and high-temperature conditions. The fidelity of the P2D-T model has been verified in many existing works (see, e.g., Li et al. (2021b)) and the procedure will thus not be repeated in the present investigation. Instead, the model parameters are obtained from the software GT AutoLion for a 2.4-Ah NMC-Graphite cell. The battery plant model is solved using the continuous-time solver `ode23ts` with guaranteed numerical stability for such a stiff system. For the controller, the same numbers of control volumes and the same model parameters as the plant are used. Under the assumption of perfect state estimation, the plant state x is sampled at $\Delta t = 1$ s.

3.2 Performance of the Proposed Inversion-Based Output Tracking for Battery Charging

An example of the simulated current profile based on the proposed inversion-based fast charging strategy is shown in Fig. 2, where the calculated input u_j^* for each constraint is also plotted and indicated by the output index j. In this example, all inequality constraints described in the previous sections are considered for demonstration purposes, although only a subset of them may be needed for a practical design. The constraints for the control are: maximum charging current rate $\overline{I}_{app}/Q_{max} = 8$C, maximum voltage $\overline{V}_{bat} = 4.4$ V, maximum charging power $\overline{P}_{bat} = 70$ W, maximum battery temperature $\overline{T} = 323.15$ K (50 °C), minimum lithium plating potential (LiP) $\eta_{LiP} = 0$ V, maximum solid-phase surface concentration $\overline{c}_{ss}^{neg} = 0.98 c_{s,max}^{neg}$,
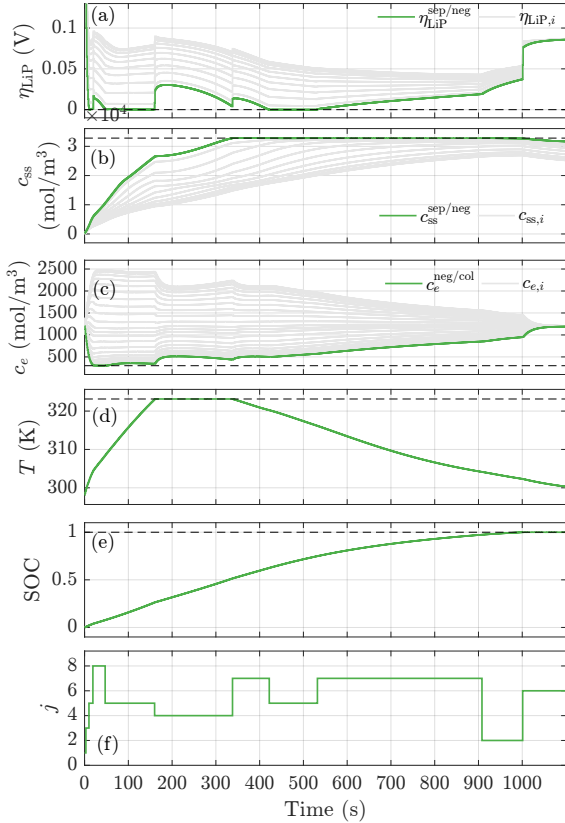
Fig. 3. Outputs as physical constraints under the proposed current profile in Fig. 2. (a) Local LiP potentials in the negative electrode. (b) Local solid-phase surface concentrations in the negative electrode. (c) Local electrolyte concentrations. (d) Battery temperature. (e) SOC. (f) Activated control mode. The dashed lines indicate the tracking references

and minimum electrolyte concentration $\underline{c}_e = 0.25c_e^0$. The battery is charged from the fully empty state to the fully charged state, i.e., $SOC_0 = 0$, $SOC_f = 1$. Furthermore, we select all the time constants as 1 s.

The simulated LiP potentials, solid-phase concentrations at particle surfaces, electrolyte concentrations, temperature, SOC, and the index of the activated output variables are shown in Fig. 3. In this example, the capability of the charging rate is limited by the current and power ($j = 1, 3$) only at the very beginning of the charging process (i.e., $t \leq 10$ s), while most of the time (10 s $< t \leq 908$ s), it is limited by the internal variables such as LiP, temperature, and concentrations ($j = 4, 5, 7, 8$). At the end of the charging process, the terminal voltage and SOC constraints play the limiting roles ($j = 2, 6$). This result demonstrates the importance of considering the internal electrochemical and thermal behaviors during fast charging, while the conventionally considered factors only have impacts at the very initial and late stages of the charging process. Furthermore, from Fig. 3(a) and Fig. 3(b), we can see the significance of considering the electrode nonuniformity in the electrode when investigating the fast charging of Li-ion batteries.

Table 1. Performance Comparison Between Different Fast-Charging Strategies

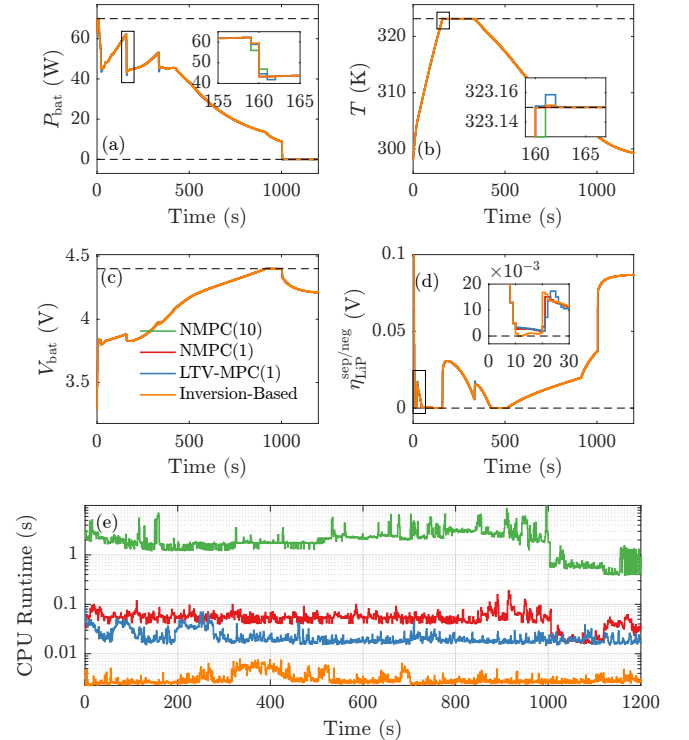|	NMPC	NMPC	LTV-MPC	Inv.-Based
Pred. horizon	10	1	1	–
Charging Time	1002 s	1002 s	1002 s	1002 s
RMSE of I_{app}	–	0.003C	0.003C	0.005C
RMSE of SOC	–	0.0001	0.0001	0.0002
MAX of SOC	–	0.0003	0.0003	0.0004
CPU runtime per 1-s sample	2.41 s	0.0576 s	0.0229 s	0.0032 s

Fig. 4. Comparison of NMPC, LTV-MPC, and the proposed inversion-based control for battery fast charging. The dashed lines represent different bounds. (a) Battery power. (b) Battery temperature. (c) Battery voltage. (d) LiP potential at the sep/neg boundary). (e) CPU runtime per sample time ($\Delta t = 1$ s)

3.3 Comparative Studies With NMPC and LTV-MPC

In this subsection, the inversion-based output tracking charging strategy is compared with MPC-based schemes. LTV-MPC and NMPC algorithms (Rawlings et al. (2017)) are used to design three charging strategies based on the same battery model and constraints: NMPC with a longer prediction of 10, one-step NMPC, and one-step LTV-MPC. Table 1 compares their numerical performances. The NM-PC is solved using the sequential quadratic programming provided by the `fmincon` function and LTV-MPC is solved using the `quadprog` in MATLAB. It shows both one-step NMPC and one-step LTV-MPC have achieved nearly the same charging time and current/SOC profiles to the NM-PC solution with a long prediction horizon. The proposed strategy is also able to achieve a very close result to the MPC strategies. However, the computational cost of the proposed strategy is much lower than the MPCs: It is over 10 and 20 times faster than the one-step LTV-MPC

and NMPC strategies, respectively. Furthermore, when the NMPC is considered as the benchmark, the root-mean-square error (RMSE) and the maximum absolute error (MAX) of the inversion-based control are close to those of MPC schemes.

4. CONCLUSIONS

In this paper, we show that if an internal or an external variable, or their first-order time derivatives, of a Li-ion battery model can be expressed in an input-affine or input-quadratic form, an inversion-based multiple-output tracking strategy can be designed for fast charging. Different physical operating limits are considered as the tracking references, and the charging current is bounded by complying with the constraint requirement when a given tracking control signal comes into action. Consequently, the charging current is explicitly expressed as a state-dependent function. The input-output control stability and performance are guaranteed by shaping the input-output relationship as a first-order linear system, and the tuning effort of the control parameters is limited to decide the corresponding time constants. The results in the illustrative examples have exhibited the computational superiority of the proposed inversion-based nonlinear control algorithm to MPC-based control algorithms. However, it should be noted that the model inversion technique requires accurate model parameters and state estimation. Thus, robustness to model uncertainty should be addressed in future investigations.

REFERENCES

Boyce, A.M., Cumming, D.J., Huang, C., Zankowski, S.P., Grant, P.S., Brett, D.J.L., and Shearing, P.R. (2021). Design of scalable, next-generation thick electrodes: Opportunities and challenges. *ACS Nano*, 15(12), 18624–18632.

Chen, L., Wu, S., Shieh, D., and Chen, T. (2013). Sinusoidal-ripple-current charging strategy and optimal charging frequency study for Li-ion batteries. *IEEE Trans. Ind. Electron.*, 60(1), 88–97.

Devasia, S. (2002). Should model-based inverse inputs be used as feedforward under plant uncertainty? *IEEE Trans. Autom. Control*, 47(11), 1865–1871.

Devasia, S., Chen, D., and Paden, B. (1996). Nonlinear inversion-based output tracking. *IEEE Trans. Autom. Control*, 41(7), 930–942.

Klein, R., Chaturvedi, N.A., Christensen, J., Ahmed, J., Findeisen, R., and Kojic, A. (2011). Optimal charging strategies in lithium-ion battery. In *Proc. Amer. Control Conf.*, 382–387.

Lee, Y. and Park, S. (2015). Electrochemical state-based sinusoidal ripple current charging control. *IEEE Trans. Power Electron.*, 30(8), 4232–4243.

Li, Y., Karunathilake, D., Vilathgamuwa, D.M., Mishra, Y., Farrell, T.W., Choi, S.S., and Zou, C. (2021a). Model order reduction techniques for physics-based lithium-ion battery management: A survey. *IEEE Ind. Electron. Mag.* doi:10.1109/MIE.2021.3100318.

Li, Y., Vilathgamuwa, D.M., Wikner, E., Wei, Z., Zhang, X., Thiringer, T., Wik, T., and Zou, C. (2021b). Electrochemical model-based fast charging: Physical constraint-triggered PI control. *IEEE Trans. Energy Convers.*, 36(4), 3208–3220. doi:10.1109/TEC.2021.3065983.

Li, Y., Vilathgamuwa, M., Farrell, T., Choi, S.S., Tran, N.T., and Teague, J. (2019). A physics-based distributed-parameter equivalent circuit model for lithium-ion batteries. *Electrochim. Acta*, 299, 451–469. doi:10.1016/j.electacta.2018.12.167.

Li, Y., Wei, Z., Xiong, B., and Vilathgamuwa, D.M. (2022). Adaptive ensemble-based electrochemical-thermal degradation state estimation of lithium-ion batteries. *IEEE Trans. Ind. Electron.*, 69(7), 6984–6996. doi:10.1109/TIE.2021.3095815.

Li, Y., Xiong, B., Vilathgamuwa, D.M., Wei, Z., Xie, C., and Zou, C. (2021c). Constrained ensemble Kalman filter for distributed electrochemical state estimation of lithium-ion batteries. *IEEE Trans. Ind. Informat.*, 17(1), 240–250. doi:10.1109/TII.2020.2974907.

Liu, J., Li, G., and Fathy, H.K. (2017). An extended differential flatness approach for the health-conscious nonlinear model predictive control of lithium-ion batteries. *IEEE Trans. Control Syst. Technol.*, 25(5), 1882–1889.

Liu, Y. and Luo, Y. (2010). Search for an optimal rapid-charging pattern for Li-ion batteries using the Taguchi approach. *IEEE Trans. Ind. Electron.*, 57(12), 3963–3971.

Moulay, E. and Perruquetti, W. (2005). Stabilization of nonaffine systems: A constructive method for polynomial systems. *IEEE Trans. Autom. Control*, 50(4), 520–526.

Notten, P.H.L., Op het Veld, J.H.G., and van Beek, J.R.G. (2005). Boostcharging Li-ion batteries: A challenging new charging concept. *J. Power Sources*, 145(1), 89–94.

Pozzi, A., Zambelli, M., Ferrara, A., and Raimondo, D.M. (2020). Balancing-aware charging strategy for series-connected lithium-ion cells: A nonlinear model predictive control approach. *IEEE Trans. Control Syst. Technol.*, 28(5), 1862–1877.

Pramanik, S. and Anwar, S. (2016). Electrochemical model based charge optimization for lithium-ion batteries. *J. Power Sources*, 313, 164–177.

Rawlings, J., Mayne, D., and Diehl, M. (2017). *Model Predictive Control: Theory, Computation, and Design.* Nob Hill Publishing.

Wang, S. and Liu, Y. (2015). A PSO-based fuzzy-controlled searching for the optimal charge pattern of Li-ion batteries. *IEEE Trans. Ind. Electron.*, 62(5), 2983–2993.

Yang, X.G. and Wang, C.Y. (2018). Understanding the trilemma of fast charging, energy density and cycle life of lithium-ion batteries. *J. Power Sources*, 402, 489–498.

Zou, C., Hu, X., Wei, Z., and Tang, X. (2017). Electrothermal dynamics-conscious lithium-ion battery cell-level charging management via state-monitored predictive control. *Energy*, 141, 250–259.

Zou, C., Hu, X., Wei, Z., Wik, T., and Egardt, B. (2018). Electrochemical estimation and control for lithium-ion battery health-aware fast charging. *IEEE Trans. Ind. Electron.*, 65(8), 6635–6645.